Journal Name

COMMUNICATION

Supramolecular coordination polymers using a close to 'V-shaped' fluorescent 4-amino-1,8-naphthalimide Tröger's base scaffold

Received 00th January 20xx,
Accepted 00th January 20xx

DOI: 10.1039/x0xx00000x

www.rsc.org/

Sankarasekaran Shanmugaraju,*[a] Chris S. Hawes,[a] Aramballi J. Savyasachi,[a] Salvador Blasco,[a] Jonathan A. Kitchen,[b] and Thorfinnur Gunnlaugsson*[a]

A V-Shaped 4-amino-1,8-napthalimide derived dipyridyl ligand comprising the Tröger's base structural motif has been synthesised and subsequently used in the formation of two new supramolecular coordination polymers.

Functional coordination polymers (CPs) have attracted tremendous attention and enormous progress has been made in the past decades, due to their intriguing structural features and potential applications.[1] CPs are typically constructed by the self-assembly of metal ions or clusters and multidentate organic bridging ligands (building blocks).[2] The structure and functionality of CPs can be systematically tailored for their specific function, by judicious choice of building blocks and reaction conditions.[3] Among diverse CPs, those constructed with nitrogen-rich open sites have drawn special attention because of their application in the context of energy and environmental-related gas adsorption and sequestration from mixed gas stream.[4] In the specific case of permanently porous coordination polymers, anchoring Lewis basic nitrogen sites into the backbone of an organic bridging linker can increase the CO_2 adsorption enthalpy and thus result in enhanced gas uptake performance at low partial pressure for these materials.[5] However, generation of CPs with Lewis basic open sites is a great challenge due to their competitive coordination with metal ions during the polymer synthesis.[6] Here we present the synthesis of two new CPs with nitrogen-rich open sites, these being based on the 4-amino-1,8-naphthalimide Tröger's (**NapTB**) base scaffold. **NapTB** are highly versatile building blocks that we have developed and employed in various supramolecular structures (*c.f.* discussion below).

The Tröger's base (TB) is a fascinating chiral molecule, comprising a methano-1,5-diazocine ring fused with two aromatic molecules almost orthogonal to each other giving rise to a unique V-shaped structure possessing a hydrophobic cavity.[7] The ease of synthesis and its unique cleft-shaped has made TBs attractive scaffolds for use in host-guest systems and in numerous supramolecular constructs.[8] The 1,8-naphthalimide derivatives belong to an important class of heterocyclic system, which absorb and emit in the visible region of spectrum.[9] Due to their strong fluorescence emission Internal charge transfer (ICT) properties, 4-amino-1,8-naphthalimides have been used in a variety of applications including as sensors for bio-related analytes and as imaging probes in bio-medicine,[10] and in the generation of diverse functional supramolecular assemblies and extended polymeric networks.[11] Over the past several years, we have merged these two functionalities within a single building block, to design new bifunctional supramolecular scaffolds and discrete compounds for use in medicinal and material chemistries.[12] Here we report the synthesis and solvatochromism of a new **NapTB** ligand **L** and its use in the formation of two new supramolecular coordination polymers: $[Co(\mathbf{L})Cl_2].2\frac{2}{3}H_2O$ (**TB-Co-CP**) and $[Cd(\mathbf{L})_2(NO_3)_{0.5}(H_2O)_{1.5}].1.5(NO_3)\cdot 4CH_2Cl_2$ (**TB-Cd-TB**). The design of **L** was based on the following rationale: i) it is fluorescent and as such can be used in sensing applications; ii) the Tröger's base motif gives rise to a cleft-shaped structure which results in an intrinsic cavity that can generate functional materials with accessible void space; iii) the flexible 3-picolylamine can lead to coordination networks with unusual topology.[1] Ligand **L** (bis-[*N*-

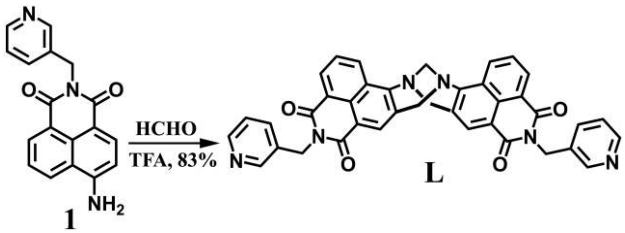

Scheme 1. Synthesis of **L**.

[a] *School of Chemistry and Trinity Biomedical Sciences Institute (TBSI), Trinity College Dublin, The University of Dublin, Dublin 2, Ireland. E-mail: shanmugs@tcd.ie; gunnlaut@tcd.ie*

[b] *Chemistry, Faculty of Natural and Environmental Sciences, University of Southampton-Highfield, Southampton, SO17 1BJ, UK.*

Electronic Supplementary Information (ESI) available: Synthesis and characterization of **2** and **L**., photophysical properties, and powder diffraction, TGA, SEM, and crystallographic details of **TB-Co-CP** and **TB-Cd-CP**. CCDC 1568817 (**TB-Co-CP**) and 1568818 (**TB-Cd-CP**). For ESI and crystallographic data in CIF format See DOI: 10.1039/x0xx00000x

(3-pyridyl)methyl)]-9,18-methano-1,8-naphthalimide-[*b,f*][1,5]diazocine) was prepared as a racemic mixture in 83% from 4-amino-1,8-naphthalimide precursor (**1**) as shown in Scheme 1 (for experimental details see ESI). **L** was fully characterised by various spectroscopy techniques such as FTIR, NMR (^{1}H and ^{13}C) and HRMS (for details see ESI). Ligand **L** was found to be highly soluble in CH_2Cl_2, THF, DMF and DMSO, but sparingly soluble in toluene and CH_3CN.

The 4-amino-1,8-naphthalimide derivatives are known to be strongly coloured and fluorescent due to the ICT, which gives rise to a large excited-state dipole moment that is solvent polarity dependent. Hence, the absorption and emission spectra of **L** were recorded in different solvents with varying polarity. The UV-Vis absorption spectra of **L** in both protic and aprotic solvents showed a high-energy transition at 345-348 nm and a low-energy band at 385-391 nm (Fig. S9, ESI). The former band is ascribed to π π* transition, while the later one is due to the ICT transition. The fluorescence emission spectra of **L** exhibited solvatochromism; being significant red-shift in the emission maxima upon increasing the solvent polarity (Fig. 1). For example, in toluene (*P* = 2.4), **L** exhibited blue emission at 469 nm, while in DMSO (*P* = 7.2), a yellow-green emission at 524 nm was observed. We also observed that the Stokes shift increased significantly from 83 to 133 nm (Table 1, ESI); this being accompanied by spectral broadening, indicating that the solvent stabilisation is more pronounced in the excited states compared to the ground states.

We then explored the coordination chemistry of **L** in the synthesis of two new coordination polymers **TB-Co-CP** and **TB-Cd-CP**. Green rod crystals of **TB-Co-CP** were obtained from the solvothermal reaction of **L** and $CoCl_2$ (1:1) in DMF at 100°C and analysed by single crystal X-ray diffraction. The data were solved and refined in the orthorhombic space group *Pnna*. The asymmetric unit contains one molecule of **L** coordinating through each pyridine nitrogen atom to two crystallographically equivalent cobalt(II) ions, whose charge is balanced by two chlorido ligands (Fig. 2). The cobalt ion adopts a distorted tetrahedral coordination geometry with an enlarged Cl1-Co1-Cl2 angle of 127.54(12)° common amongst Cl2N2 four-coordinate cobalt(II) species (*c.f.* Fig. S10, ESI).[13] The two nitrogen atoms coordinate at Co-N distances 2.040(7) and 2.113(6) Å for N1 and N6, respectively, though slight crystallographic disorder on the pyridine ring of N6 makes the former value somewhat unreliable. The **L** molecule adopts the expected cleft conformation between the two naphthalimide rings, with a mean inter-planar angle between the naphthalene fragments of 81.1°. Both pyridine groups are twisted inwards towards the centre of the cleft, providing a relatively short bridging distance between the two cobalt ions of 10.533(3) Å (Fig. 2). The extended structure of **TB-Co-CP** is a one-dimensional coordination polymer, oriented parallel to the *a* axis. The cleft shape of **L** and inwards-facing of pyridine groups impart a *zig-zag* nature to the polymeric assembly with oscillations in the *b* direction. Adjacent chains interact by way of offset face-to-face π-π interactions between the naphthalimide groups (Fig. 2). Each of the two unique naphthalimide groups interact with their symmetry equivalents to link the chains into the *b* and *c* directions. The most substantial interaction takes place between the outer faces of two naphthalimide groups at a mean interplanar angle of 2.8° and with minimum inter-atomic distance of 3.537(10) Å for C32···C32, linking chains in the *b* direction (Fig. S11, ESI). The two naphthalimide rings involved in this interaction are aligned in a nearly head-to-head fashion, with a twist of *ca*. 30° between the major axes of each group. An additional head-to-tail interaction is observed on the opposite faces of each molecule, with only a minor overlap between the two planes and minimum inter-atomic distance of 3.475(7) Å for C31···C29. A similar interaction between the outer faces of each

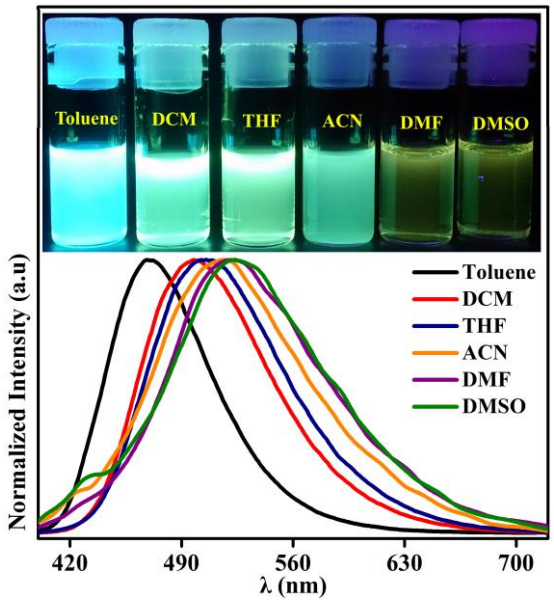

Fig. 1. Normalized fluorescence emission spectra of **L** (24 μM) in different solvents with varying polarity (Inset: corresponding photographs).

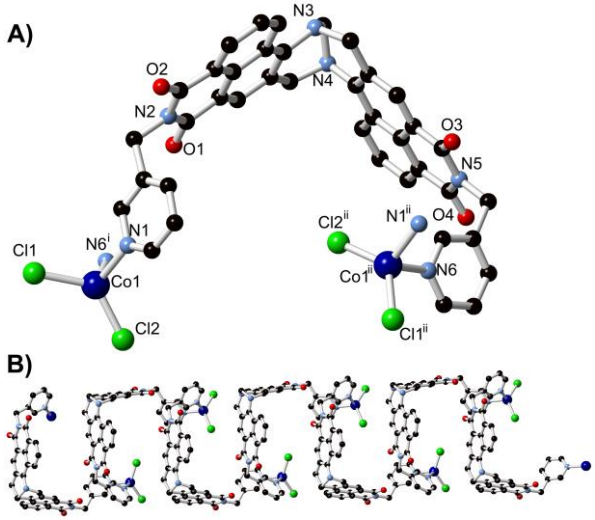

Fig. 2. (A) Structure of complex **TB-Co-CP** with partial labelling scheme. (B) Extended structure of a single chain of complex **TB-Co-CP** viewed parallel to the crystallographic *b* axis. Heteroatoms and pyridyl ring disorder are omitted for clarity. Symmetry codes used to generate equivalent atoms: (i) ½+X, +Y, ½-Z; (ii) X-½, +Y, 1-Z.

naphthalimide group occurs between chains linked in the *c* direction, however no strong interactions were observed with the inner face of this naphthalimide group, which is oriented towards an area of diffuse electron density which could not be assigned crystallographically (Fig. S11, ESI). By elemental analysis, the content of these channels was best fitted as $2\frac{2}{3}H_2O$ molecules per [$CoCl_2$(**L**)] formula unit, comprising 6 wt%. The solvent-accessible volume calculated by SQUEEZE of *ca.* 175 Å^3 and 58 electrons per formula unit (Z = 8), would indicate the as-synthesised material is likely to contain additional solvent molecules which are lost upon isolation and drying of the material in air, which is also consistent with the broad and poorly crystalline appearance of the X-ray powder diffraction pattern (Fig. S12, ESI). Thermogravimetric analysis reveals a complex multi-step thermal decomposition pathway for the freshly isolated sample; an initial mass loss of 8% occurs in the range 30–130 °C, before a more gradual loss of a further 9% below 300 °C, presumably representing a mixture of mobile and poorly mobile solvent molecules within the freshly isolated framework which are lost on extended standing in air, above 300°C, decomposition of the remaining organic fraction of the framework is observed (Fig. S13, ESI).

Single crystals of complex **TB-Cd-CP** were obtained by slow evaporation from the reaction mixture of **L** and $Cd(NO_3)_2.4H_2O$ in DCM/CH_3OH/CH_3CN (*v/v*, 1:1:1) solvent mixture, and analysis by single crystal X-ray diffraction provided a structural model in the monoclinic space group $P2_1/c$. The asymmetric unit contains two unique molecules of **L** and two cadmium ions, both occupying crystallographic special positions (Fig. 3). The associated nitrate counterions exhibit significant positional disorder; the best fit was obtained by modelling one full occupancy non-coordinating nitrate anion, with the remaining nitrate anion modelled in a mixture of coordinating and non-coordinating positions. The two cadmium ions both adopt centrosymmetric octahedral coordination geometries with four equatorially oriented pyridyl ligands, with the axial positons occupied by aqua ligands (Cd1) or a disordered mixture of aqua ligands and nitrato ligands (Cd2, see Fig. 3). Each of the two ligand molecules bridges two cadmium ions with a metal-metal distance of 9.9857(3) Å. This distance is marginally shorter than the equivalent distance in complex **TB-Co-CP** (10.533(3) Å), indicative of the more compact folded conformation adopted by the ligands in complex **TB-Cd-CP**. A substantial fraction of the unit cell was found to contain heavily disordered solvent molecules characterised by diffuse Fourier residuals which could not be realistically modelled, and as such, the SQUEEZE routine within PLATON was employed to account for these guests. The predicted electron count (183 e- per Cd ion) is reasonably well-matched by the bulk formulation determined by elemental analysis, *poly*-[Cd(**L**)$_2$(NO_3)$_{0.5}$(H_2O)$_{1.5}$]1.5(NO_3)·4CH_2Cl_2, which gives an expected unresolved electron count of 168 e- per Cd ion. When extended by crystallographic symmetry, complex **TB-Cd-CP** exhibits a one-dimensional polymeric structure oriented parallel to the crystallographic 101 vector. The chain itself consists of two in-phase coaxial *zig-zags* with amplitude vectors oriented approximately 66° from one another, each associated with a crystallographically unique **L** molecule (Fig. 4). Adjacent chains interact through myriad face-to-face π-π stacking interactions between the outer naphthalimide faces, which exhibit average (naphthalimide) centroid···centroid distances of 3.34 Å and inter-atomic distances of similar magnitudes, indicative of significant attractive forces (Fig. 4). These interactions link each chain of **TB-Cd-CP** to four other parallel chains, leaving solvent channels parallel to the polymer axis within which the bulk of the diffuse lattice solvent molecules are expected to reside (Fig. S14, ESI). Thermogravimetric analysis of an air-dried sample revealed very little volatile mass remained following isolation of the crystals (3% mass loss below 75 °C), indicating a rapid desolvation process (Fig. S15, ESI); X-ray powder diffraction of the dry sample showed only amorphous features, indicating this rapid desolvation process is accompanied by a complete loss of crystallinity (Fig. S16, ESI). CP-MAS ^{13}C NMR analysis shows the expected carbon-resonances corresponding to **L** in the range of 40-163 ppm for the degraded material (Fig. S17, ESI). The emission properties of

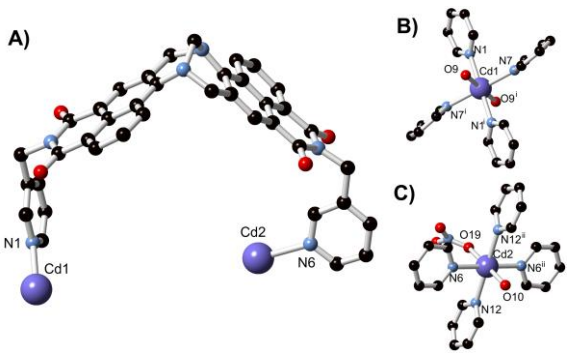

Fig. 3. (A) Representative example of ligand geometry in complex **TB-Cd-CP** (one of two unique ligand molecules shown, for clarity) with partial atom labelling scheme. (B, C) The coordination environment of the two cadmium ions in complex **TB-Cd-CP** with labelling scheme for coordinating atoms. Hydrogen atoms, and aqua/nitrate substitutional disorder for Cd2 are omitted for clarity. Symmetry codes used to generate equivalent atoms: (i) 2-x, 1-y, 1-z; (ii) 1-x, 1-y, -z.

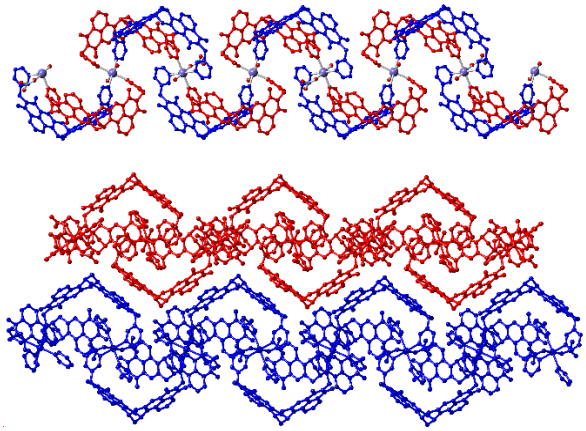

Fig. 4. (Top) Extended structure of a single chain of **TB-Cd-CP** with symmetry-related **L** groups coloured together, showing the two-overlapping zig-zag chains present within the structure; (Bottom) Face-to-face π-π interactions between two adjacent chains of **TB-Cd-CP**, with separate chains coloured independently.

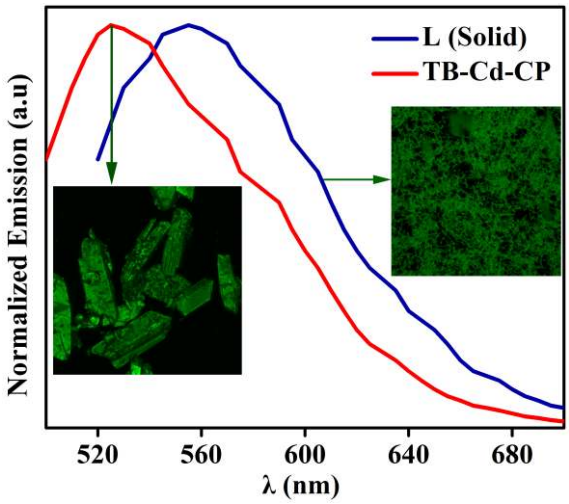

Fig. 5. Solid-state emission spectra for complex **TB-Cd-CP** (λ_{max} = 525 nm) compared to free ligand **L** (λ_{max} = 555 nm) (Inset: corresponding confocal fluorescence microscopy images).

degraded **TB-Cd-CP** material are also closely related to the behaviour observed for **L** itself when immersed in various organic solvents, which most likely contain a continuum of unbound **L** molecules and various [Cd**L**] oligomers and aggregates (Fig S19, ESI).

To examine the morphological features of the materials, we performed Scanning Electron Microscopy (SEM) analysis, which demonstrated that **TB-Co-CP** exhibits a typical rod morphology, while **TB-Cd-CP** consist of large rectangular block-shaped particles (Fig. S17, ESI). The solid-state emission spectra of **L** displayed a broad emission band centred at λ_{em} = 555 nm, which is assigned to the "push-pull" ICT transition. The emission spectra of complex **TB-Cd-CP** exhibited a structurally similar band at λ_{em} = 525 nm, which is *ca.* 30 nm blue-shifted compared to the emission of **L**. The observed hypsochromic shift of **TB-Cd-CP** in the solid state is due to the strong electronic coupling through coordination as well as to the difference in the mode of aggregation between **L** and **TB-Cd-CP** in the solid-state. The fluorescence microscopy image of drop-cast sample of **L** and **TB-Cd-CP** displayed a prominent green emission (Fig. 5).

In summary, we have synthesized two new coordination polymers **TB-Co-CP** and **TB-Cd-CP**, containing Tröger's base structural motifs, from a new V-shaped 4-amino-1,8-naphthalimide derived Tröger's base luminescent scaffold **L**. These are the second examples of such systems, and the first to be structurally characterised through X-ray diffraction analysis, which demonstrated that, in each case, substantial face-to-face π–π interactions prevail the extended structures, leading to 1D-supramolecular polymeric networks. These results are of major importance in demonstrating the application of **NapTB** in coordination and inorganic supramolecular chemistry.

We thank the Irish Research Council (IRC) for a postdoctoral fellowship (GOIPD/2013/442 to S.S and GOIPD/2015/446 to C.S.H), Marie Skłodowska-Curie actions (MSCA) Incoming Fellowship (to SB), and Science Foundation Ireland (SFI PI Award 13/IA/1865 to TG), for financial support. We thank Dr. Gavin J. McManus (TBSI) for helping with confocal fluorescence imaging experiments and Dr. Manuel Ruether for the solid-state ^{13}C-NMR experiment.

Notes and references

1. Y. Cui, B. Li, H. He, W. Zhou, B. Chen and G. Qian, *Acc. Chem. Res.*, 2016, **49**, 483; W. P. Lustig, S. Mukherjee, N. D. Rudd, A. V. Desai, J. Li and S. K. Ghosh, *Chem. Soc. Rev.*, 2017, **46**, 3242.
2. Y. Cui, Y. Yue, G. Qian and B. Chen, *Chem. Rev.*, 2012, **112**, 1126; H. Furukawa, K. E. Cordova, M. O'Keeffe and O. M. Yaghi, *Science*, 2013, **341**, 1166; G. R. Newkome and C. N. Moorefield, *Chem. Soc. Rev.*, 2015, **44**, 3954.
3. A. J. Howarth, A. W. Peters, N. A. Vermeulen, T. C. Wang, J. T. Hupp and O. K. Farha, *Chem. Mater.*, 2017, **29**, 26; A. K. Crane, N. G. White and M. J. MacLachlan, *CrystEngComm*, 2015, **17**, 4912; G. Tobin, S. Comby, N. Zhu, R. Clerac, T. Gunnlaugsson and W. Schmitt, *Chem. Commun.*, 2015, **51**, 13313.
4. J. Jiao, L. Dou, H. Liu, F. Chen, D. Bai, Y. Feng, S. Xiong, D.-L. Chen and Y. He, *Dalton Trans.*, 2016, **45**, 13373; A. Demessence, D. M. D'Alessandro, M. L. Foo and J. R. Long, *J. Am. Chem. Soc.*, 2009, **131**, 8784.
5. S. Seth, G. Savitha and J. N. Moorthy, *Inorg. Chem.*, 2015, **54**, 6829; B. Gole, A. K. Bar, A. Mallick, R. Banerjee and P. S. Mukherjee, *Chem. Commun.*, 2013, **49**, 7439; Y. Li, Z. Jiang, J. Yuan, D. Liu, T. Wu, C. N. Moorefield, G. R. Newkome and P. Wang, *Chem. Commun.*, 2015, **51**, 5766.
6. A. Chakraborty, S. Roy, M. Eswaramoorthy and T. K. Maji, *J. Mater. Chem. A*, 2017, **5**, 8423; T. Panda, P. Pachfule, Y. Chen, J. Jiang and R. Banerjee, *Chem. Commun.*, 2011, **47**, 2011.
7. Ö. V. Rúnarsson, J. Artacho and K. Wärnmark, *Eur. J. Org. Chem.*, 2012, **2012**, 7015; S. Shanmugaraju, D. McAdams, F. Pancotti, C. S. Hawes, E. B. Veale, J. A. Kitchen and T. Gunnlaugsson, *Org. Biomol. Chem.*, 2017, **15**, 7321.
8. T. Weilandt, U. Kiehne, J. Bunzen, G. Schnakenburg and A. Lützen, *Chem. Eur. J.*, 2010, **16**, 2418; Y.-M. Jeon, G. S. Armatas, D. Kim, M. G. Kanatzidis and C. A. Mirkin, *Small*, 2009, **5**, 46.
9. H. Izawa, S. Nishino, M. Sumita, M. Akamatsu, K. Morihashi, S. Ifuku, M. Morimoto and H. Saimoto, *Chem. Commun.*, 2015, **51**, 8596; C. S. Hawes, K. Byrne, W. Schmitt and T. Gunnlaugsson, *Inorg. Chem.*, 2016, **55**, 11570.
10. S. Banerjee, E. B. Veale, C. M. Phelan, S. A. Murphy, G. M. Tocci, L. J. Gillespie, D. O. Frimannsson, J. M. Kelly and T. Gunnlaugsson, *Chem. Soc. Rev.*, 2013, **42**, 1601; M. Li, H. Ge, R. L. Arrowsmith, V. Mirabello, S. W. Botchway, W. Zhu, S. I. Pascu and T. D. James, *Chem. Commun.*, 2014, **50**, 11806.
11. T. Weilandt, U. Kiehne, G. Schnakenburg and A. Lutzen, *Chem. Commun.*, 2009, 2320; J. I. Lovitt, C. S. Hawes, A. D. Lynes, B. Haffner, M. E. Mobius and T. Gunnlaugsson, *Inorg. Chem. Front*, 2017, **4**, 296; J. A. Kitchen, P. N. Martinho, G. G. Morgan and T. Gunnlaugsson, *Dalton Trans.*, 2014, **43**, 6468; D. L. Reger, A. Leitner and M. D. Smith, *Crys. Growth Des.*, 2015, **15**, 5637; J. K. Nath and J. B. Baruah, *CrystEngComm*, 2015, **17**, 8575; J. A. Kitchen, N. Zhang, A. B. Carter, A. J. Fitzpatrick and G. G. Morgan, *J. Coord. Chem.*, 2016, **69**, 2024.
12. E. B. Veale and T. Gunnlaugsson, *J. Org. Chem.*, 2010, **75**, 5513; S. Shanmugaraju, C. Dabadie, K. Byrne, A. J. Savyasachi, D. Umadevi, W. Schmitt, J. A. Kitchen and T. Gunnlaugsson, *Chem. Sci.*, 2017, **8**, 1535.
13. I. J. Bruno, J. C. Cole, P. R. Edgington, M. Kessler, C. F. Macrae, P. McCabe, J. Pearson and R. Taylor, *Acta Cryst. B*, 2002, **58**, 389; C. R. Groom, I. J. Bruno, M. P. Lightfoot and S. C. Ward, *Acta Cryst. B,* 2016, **72**, 171.

